Design, Preparation, and Characterization of a Novel Hyper-Cross-Linked Polyphosphamide Polymer and Its Adsorption for Phenol

ARTICLE *in* INDUSTRIAL & ENGINEERING CHEMISTRY RESEARCH · SEPTEMBER 2011

Impact Factor: 2.59 · DOI: 10.1021/ie201412s

6 AUTHORS, INCLUDING:

Hong Jiang
University of Science and Technology of China
55 PUBLICATIONS **641** CITATIONS
SEE PROFILE

Han-Qing Yu
University of Science and Technology of China
508 PUBLICATIONS **11,014** CITATIONS
SEE PROFILE

Qing-Xiang Guo
University of Science and Technology of China
262 PUBLICATIONS **6,973** CITATIONS
SEE PROFILE

I&EC research
Industrial & Engineering Chemistry Research

ARTICLE

pubs.acs.org/IECR

Design, Preparation, and Characterization of a Novel Hyper-Cross-Linked Polyphosphamide Polymer and Its Adsorption for Phenol

Fan-Xin Zeng,[†,‡] Wu-Jun, Liu,[†] Shi-Wei, Luo,[†] Hong Jiang,[†,*] Han-Qing Yu,[†] and Qing-Xiang Guo[†]

[†]Department of Chemistry, University of Science and Technology of China, Hefei 230026, P.R. China

[‡]Key Laboratory of Cellulose and Lignocellulosics Chemistry, Guangzhou Institute of Chemistry, Chinese Academy of Sciences, Guangzhou 510650, China

Supporting Information

ABSTRACT: Polar organic compounds (POCs) are one of the main categories of pollutants in wastewater, and their effective removal is highly desirable. In this work a novel hyper-cross-linked polyphosphamide resin (HPR) with flexible structure and functional groups for POCs adsorption was synthesized and characterized by Fourier transform infrared (FTIR) spectroscopy, thermogravimetric analysis (TGA), X-ray photoelectron spectroscopy (XPS), and scanning electron microscopy (SEM). Phenol, a typical POC, was used to test its adsorption amount. The experimental results showed that the polymer exhibited an excellent phenol adsorptive capacity of 516 mg g^{-1} in phenol aqueous solution, though its surface area was 14.5 m^2 g^{-1} only. The influences of pH, contact time, and the zero point charges of adsorption were investigated. This research provides a new and effective approach to separate and recover phenols, especially at a high concentration, from wastewater.

1. INTRODUCTION

Human activities (e.g., industries and municipalities) use about 10% of the globally accessible water resources and generate a large amount of wastewater, which contains numerous chemical compounds at varying concentrations.[1] Polar organic compounds (POCs), e.g., antibiotics, phenols, and amines, one of the main categories of pollutants in wastewater, are usually highly poisonous and can cause adverse health effects on animal life and humans. Effective separation and recovery of POCs from wastewater is environmentally benign and economically beneficial when the POCs are of a high level.[2]

To remove POCs, a variety of treatment technologies have been applied, including activated carbon adsorption,[3−5] advanced oxidation processes,[6−8] biodegradation,[12] etc. The selective recovery of POCs from wastewater based on the chemical interactions between some specially designed chemicals and POCs is a promising approach and has been well investigated.[9−11] The chemicals with hydroxyl and amino groups are found to have strong interactions with POCs via hydrogen bonding and can be employed as a liquid extractant to remove POCs from wastewater.[12−15] Recently, solid polymers with the similar functional groups have attracted increasing interests in the recovery of POCs from wastewater, attributed to their favorable physicochemical stability, large adsorption capacity, good selectivity, and structural diversity.[16−18] A variety of adsorptive resins were developed by grafting different groups (e.g., hydroxyl, amino, and carboxyl groups) as hydrogen bonding acceptors/donors onto the polymer matrices.[19−21] Among these, functionalized polystyrene resin is one of the largest and most important families of adsorptive resins and exhibits excellent performance for POC removal.[22,23] Theoretically, due to the electronic effect, the relatively rigid structure of the polystyrene matrix causes incomplete utilization of the grafted functional groups.[24] Compared with the resin with a rigid structure, a hyper-cross-linked polyphosphamide resin with flexible structure has many advantages. On the one hand, the phosphoryl groups (P═O) in the resin can act as adsorptive functional groups similar to those in liquid extractants.[25,26] On the other hand, a flexible structure of the resin can facilitate its stretching and rotation, thus increasing the amount of functional groups exposed to POCs and enhancing the adsorption capacity.[27] In addition, the hyper-cross-linked polyphosphamide structure is highly resistant to oxidation, which ensures a good stability of the resin.

Herein, a hyper-cross-linked polyphosphamide resin (HPR) containing phosphoryl groups (P═O) with flexible structure was synthesized. Phenol, a typical POC, was selected as a model compound to evaluate its adsorption capacity and to explore its adsorption mechanism. The main objectives of this study are as follows: (1) to design and prepare a new type of polyphosphamide resin with flexible structure; (2) to investigate the features of the resin by a series of characterizations; and (3) to compare the adsorption capacity of the resin with traditional adsorbents. The resin design approach developed in this study can find its further applications in selective recovery of POCs from wastewater.

2. MATERIALS AND METHODS

2.1. Materials. All chemicals used in this study were of analytical grade. Phenol, hexane-1,6-diamine, and Amberlite XAD-4 resin were purchased from J&K Chemical Co., Ltd., China. Phosphoryl trichloride was obtained from Alfa Aesar A Johnson Matthey Co., Ltd., China. Other solvents and reagents were purchased from Sinopharm Chemical Reagent Co., Ltd.

Received: July 2, 2011
Accepted: September 16, 2011
Revised: September 15, 2011
Published: September 16, 2011

dx.doi.org/10.1021/ie201412s | *Ind. Eng. Chem. Res.* 2011, 50, 11614–11619

China. Phosphoryl trichloride was distilled under reduced pressure before use, and other solvents and reagents were dried with appropriate drying agents.

2.2. Preparation of the HPR. The synthetic route of the HPR is shown in Figure 1. Hexane-1,6-diamine was dissolved in anhydrous dichloromethane in the presence of triethylamine in a three-neck flask equipped with a mechanical stirring device and gas outlet. The flask was then cooled in an ice−water bath for 10 min. Stirred vigorously, phosphoryl trichloride diluted by dichloromethane was carefully added in via a dropping funnel. Continuous stirring was maintained throughout the reaction period of 8 h. The resultant crude product was filtered and washed with water and methanol successively to remove the triethylamine hydrochloride and other impurities. Then the solid was extracted with acetone in a Soxhlet extractor and dried in vacuum at 353 K for 24 h. Finally, the dried HPR was crushed by a high-speed rotary cutting mill, and the particles with the size between 0.15 and 0.30 mm were collected and stored for further use.

2.3. Characterization of the HPR. Structural features of the HPR were obtained from nitrogen adsorption−desorption isotherms, carried out at 77 K using a Micromeritics Gemini apparatus (ASAP 2020 M+C, Micromeritics Co. USA). Specific surface area was obtained by the BET method, and total pore volume was calculated by the amount of nitrogen adsorbed at a relative pressure of 0.99. The HPR sample was mixed with KBr in a mass ratio of 1:100, then compressed into films, and scanned by a FTIR spectrometer (EQUINOX55, Bruker Inc., Germany) in a wavenumber range of 4000−400 cm^{-1} to analyze its functional groups. The surface morphology of the HPR was characterized by scanning electron microscopy (SEM, Sirion 200, FEI Electron Optics Co., USA). The thermal stability of HPR was characterized with a DTG-60H/DSC-60 thermogravimetric analyzer (Shimadzu Co., Japan) under N_2 atmosphere, with a heating rate of 10 K min^{-1} from room temperature to 1073 K, before TGA run, the sample was vacuum-dried at 338 K for 12 h. The surface composition and chemical state of HPR was analyzed by X-ray photoelectron spectroscopy (XPS). The XPS measurements were carried out using a Thermo VG-Scientific X-ray photoelectron spectrometer (U.K.) with a monochromatized Al Kα radiation (1486.92 eV) and in a Constant Analyzer Energy (CAE) mode with 70 eV pass energy for survey spectra and 20 eV for high resolution spectra. The intensity of the XPS peak was recorded as counts per second (CPS). The XPS peaks were deconvoluted into subcomponents using a Gaussian (80%)-Lorentzian (20%) curve-fitting program (XPSPEAK 4.1), with a Shirley type background. The pH of zero point charge (pH_{PZC}) of HPR was also measured (see Figure S1 of SI).

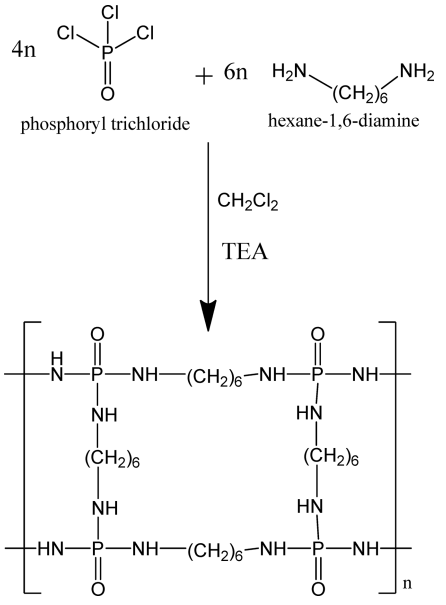

Figure 1. Scheme for the synthesis of HPR.

2.4. Phenol Adsorption Experiments. The adsorption experiments were carried out at 313 K. Dry resin samples were exactly weighed and added into 250-mL conical flasks, and 100 mL of phenol aqueous solution of different concentrations was introduced into each flask. The flasks were filled with nitrogen at 0.8 L min^{-1} for 2 min to eliminate the influence of air on phenol adsorption, then sealed, and placed in a constant-temperature oscillator at 313 K and shaken for over 24 h to reach the adsorption equilibrium. Subsequently, the suspension liquid was filtered. The residual phenol concentration of the aqueous filtrate was determined by a UV−vis spectrophotometer (UV-2401, Shimadzu Co., Japan) at a wavelength of 510 nm.[28] The adsorption amount was calculated with eq 1

$$q_e = \frac{V(C_0 - C_e)}{W} \quad (1)$$

where q_e (mg g^{-1}) is the phenol adsorption amount, V (L) is the volume of solution, W (g) is the weight of dry resin, *and* C_0 and C_e (mg L^{-1}) denote the initial and equilibrium concentrations of phenol, respectively.

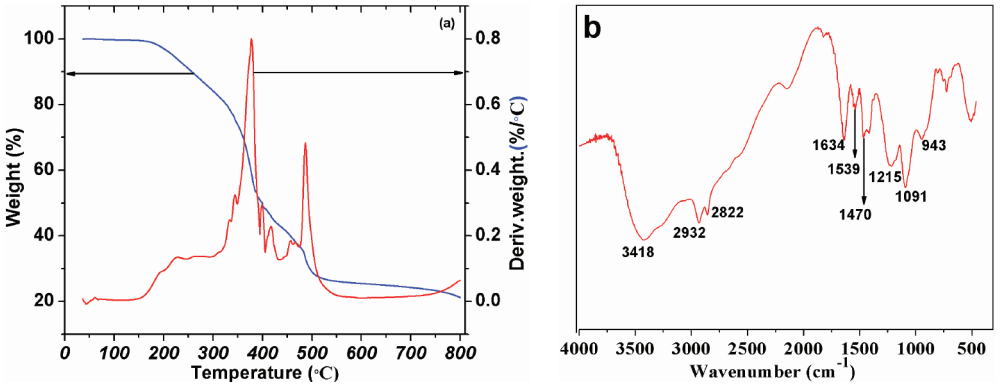

Figure 2. (a) Thermogravimetric analysis (TGA) of the HPR and (b) FTIR spectrum of the HPR.

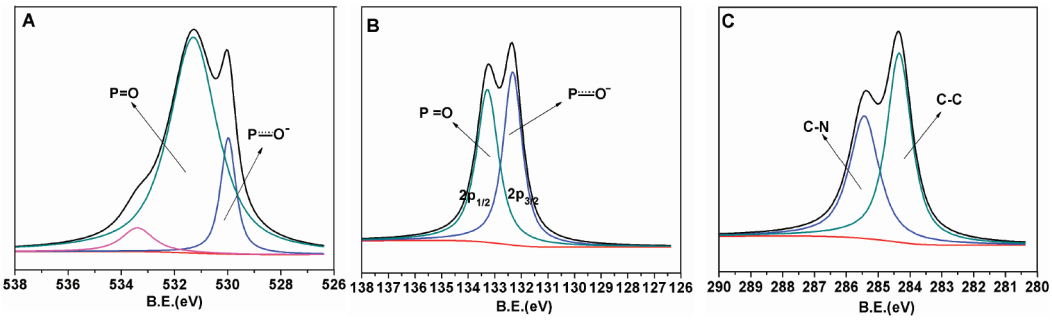

Figure 3. XPS spectra of the HPR: (A), O 1s spectrum; (B) P 2p spectrum; and (C) C 1s spectrum.

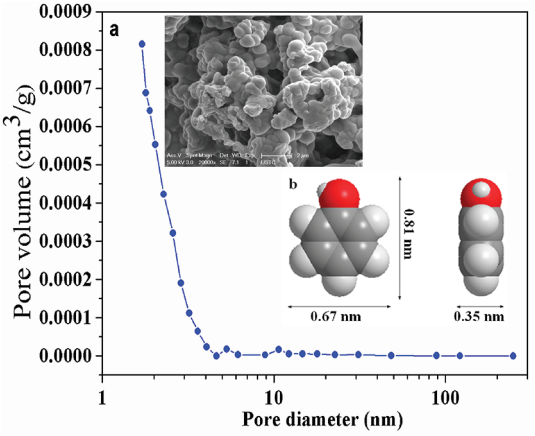

Figure 4. (a) Surface analysis of the HPR by the BET method, inset figure: SEM image (20000 ×) of the HPR; and (b) size of phenol molecule simulated with software ACDLABS 11.0.

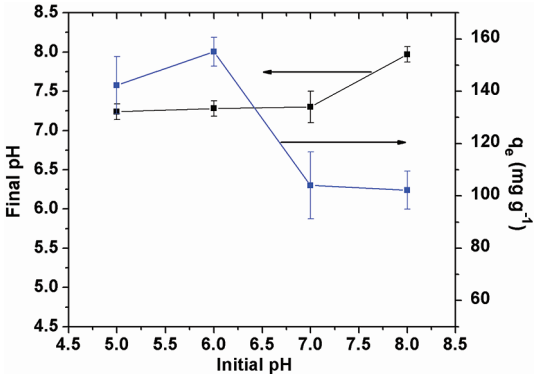

Figure 5. Influence of pH on the phenol adsorption amount of HPR (initial phenol concentration: 5000 mg L^{-1}; HPR dose, 2.0 g L^{-1}; contact time, 24 h).

3. RESULTS AND DISCUSSION

3.1. Characteristics of the HPR. The thermal degradation behavior of HPR is shown in Figure 2a. The weight loss of the HPR starts at 120 °C, and only 2.9% of the total weight was lost at temperature below 200 °C, indicating that the HPR has a high thermal stability. There are two major degradation peaks in the DTA curve. One is from ~303 to 405 °C, and 35.5% of the total weight was lost during this stage, which is attributed to the decomposition of the P−N, C−N, and P═O groups to form some volatile components (e.g., NO_x, NH_3, CO, and HCNO). The other is from 479 to 551 °C, and 10.1% of total weight was lost during this stage, which is attributed to the carbonization of the polymer (e.g., the cleavage of C−H and C−C bonds).

The IR spectrum of the synthesized HPR is shown in Figure 2b. The broad band at 3418 cm^{-1} indicated the existence of N−H, and the doublet peaks appeared at 2932 cm^{-1} and 2822 cm^{-1} were ascribed to the symmetric and asymmetric stretching of alkyl C−H. The band at 1634 cm^{-1} was the stretching of phosphoryl group (P═O). The peaks at 1539 and 1470 were the deformation vibration of N−H and bending vibration of C−H, respectively. The peaks at 1215 and 1091 cm^{-1} were attributed to the symmetric and asymmetric stretching vibration of C−N, while at 943 cm^{-1} signified the presence of P−N.[29] All these peaks found in the FTIR spectrum suggest the phosphoramide structure of the resin is formed in consistence with our design.

The chemical state of the surface elements of the HPR is analyzed using XPS. As expected, the survey spectrum (Figure S3 of SI) shows the presence of carbon (C), oxygen (O), nitrogen (N), and phosphorus (P) on the surface of HPR. To further investigate the chemical state of the surface functional groups, high resolution spectra of O 1s, P 2p, and C 1s (Figure 3 (A)-(C)) and N1s (Figure S3 of SI) are obtained. The peak at 531.3 eV of O 1s spectrum is attributed to oxygen double bonded phosphorus (O═P).[30]

As shown in Figure 4a, micropores as well as a spot of mesopores dominated the pore structure of the HPR, while macropores were negligible. Considering its extraordinary high cross-linking degree, such a result is reasonable. More details about the surface structures of the HPR could be found in the SI (Table S1). The specific surface area of the HPR was 14.5 $m^2\ g^{-1}$, and its average pore size was 2.59 nm, which is sufficiently large for the entrance of phenol molecules (Figure 4b). Accordingly, it is reasonable to assume that all the surface area of the resin could be occupied by phenol molecules. It is assumed that phenol molecules stacked with the minimum facet of 0.67 nm × 0.35 nm to keep the largest molecule amount on the HPR surface, correspondingly, the total surface area of 1 g of HPR (14.5 m^2) can accommodate 9.65 mg of phenol for one-layer stacking according to eq 2

$$W_{phenol} = \frac{S_{HPR} \times M_{phenol}}{A_{phenol} \times N_A} = \frac{14.5 \times 94000}{0.67 \times 0.35 \times 10^{-18} \times 6.023 \times 10^{23}} = 9.65\ \text{mg}\cdot\text{g}^{-1} \quad (2)$$

where A_{phenol} (m^2), W_{phenol} (mg g^{-1}), and M_{phenol} (mg mol^{-1}) are the surface area of each phenol molecule, the weight of adsorbed phenol, and the molecular weight of phenol, respectively. S_{HPR} ($m^2\ g^{-1}$) is the total surface area of the HPR, and N_A (mol^{-1}) is Avogadro's constant.

dx.doi.org/10.1021/ie201412s |Ind. Eng. Chem. Res. 2011, 50, 11614–11619

3.2. Phenol Adsorption Behavior and Mechanism of HPR.

Influence of solution pH. Solution pH is a key factor influencing the adsorption process. It not only affects the states of the functional groups on the surface of the HPR but also the existing form of the phenol in solution. Figure 5 shows the effect of pH on the phenol adsorption by HPR. It is observed that the phenol adsorption amount increases from 142 to 155 mg g^{-1} in the pH range of 5.0−6.0, showing a maximum value at pH 6.0. With further increase in pH to 7.0 and 8.0, the adsorption amount sharply decreases to 104 and 102 mg g^{-1}, respectively. This can be explained as follows: At low pH, both the phenol molecules and the functional groups of the resin are protonated and positively charged. Because of the electrostatic repulsion effect, the phenol molecules are hard to be sorbed by the functional groups of the resin, thus decreasing the adsorption amount. Such an electrostatic repulsion effect also exists in high pH value when both the phenol molecules and the functional groups of the resin are negatively charged. When at certain favorable pH values (about pH 6 in this work), the phenol molecules and the functional groups of the resin charge with different electric charges, and there is electrostatic attracting between them, thus the adsorption efficiency increases.

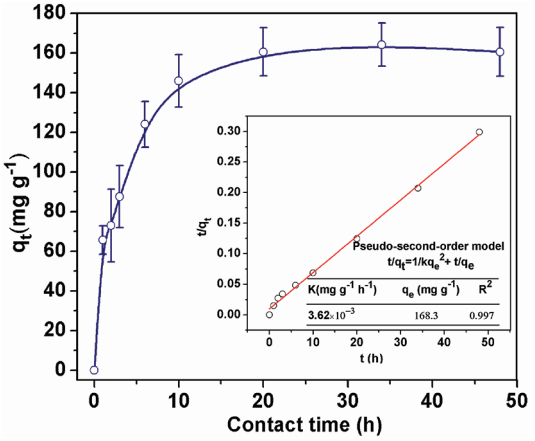

Figure 6. Phenol adsorption by the HPR in aqueous solutions at different contact time, and inset figure, pseudosecond-order kinetic models used for simulating the adsorption process (initial phenol concentration, 5000 mg L^{-1}, HPR dose, 2.0 g L^{-1}, initial pH, 6.0).

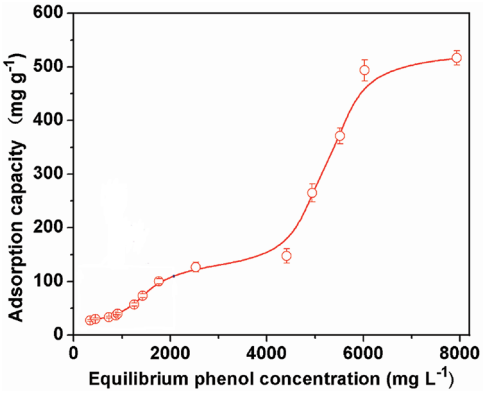

Figure 7. Phenol adsorption by HPR in aqueous solutions at initial phenol concentrations of 400−10,000 mg L^{-1}.

Influence of Contact Time. Figure 6 shows the effect of contact time on adsorption of phenol by HPR. The phenol adsorption capacities (q_t) at different time intervals ranging from 0 to 48 h are obtained. It is observed that equilibrium is achieved within approximate 20 h. The kinetics data are fitted by pseudosecond-order model expressed by eq 3[31]

$$\frac{t}{q_e} = \frac{1}{K_2 q_e^2} + \frac{1}{q_e} t \qquad (3)$$

where q_t and q_e (mg g^{-1}) are the amount of phenol adsorbed on HPR at time t (min) and equilibrium, respectively; and K_2 (g mg^{-1} h^{-1}) is the corresponding adsorption rate constant. Parameters of the pseudosecond-order model are calculated from the intercept and slope of the t/q_t versus t plot (inset figure of Figure 6). The correlation coefficient (R^2) is more than 0.99. The equilibrium adsorption amount calculated by this model ($q_{e.cal}$ = 168 mg g^{-1}) is close to that obtained from experiments ($q_{e.exp}$ = 162 mg g^{-1}), confirming the validity of the pseudosecond-order model which is based on the hypothesis that chemical sorption is the rate-limiting step of the adsorption process.[32]

Phenol Adsorption Amount and Mechanism of HPR. A series of phenol adsorption experiments were carried out to evaluate the actual adsorption amount of the HPR. As shown in Figure 7, at an initial concentration of phenol below 7000 mg L^{-1}, the phenol-adsorption amount of the HPR was slightly enhanced with an increase in phenol concentration. At an initial phenol concentration of 8000 mg L^{-1}, however, a remarkable improvement in the phenol-adsorption amount of HPR was observed. When the phenol concentration exceeded 11,000 mg L^{-1}, the adsorption equilibrium was not reachable because the HPR became viscous and was difficult to be separated from the solution. Thus, the largest adsorption amount in this experiment was 516 mg g^{-1}, which is much higher than the results calculated based on the one-layer surface physical adsorption (9.65 mg g^{-1}). The adsorption amount of HPR is higher than those of most traditional adsorbents (Table 1).[33−38]

An adsorption mechanism based on the hydrogen bonding interaction between phenol and the functional groups of the resin

Table 1. Comparison of the Adsorption Amount of HPR with Other Adsorbents Reported in the Literature

adsorbent	C_0 (mg L^{-1})	q_{max} (mg g^{-1})	reference
activated carbon fibers	0−141	110	33
magnetic polysulfone microcapsules containing tributyl phosphate	99−1050	79	34
carbonylated hyper cross-linked polymeric adsorbent	0−600	174	35
β-cyclodextrin epichlorohydrin copolymer chitosan	20−300	132	36
activated carbon from wood particleboard wastes	400	593	37
polyacrylonitrile based activated carbon	470	77	38
hyper-cross-linked polyphosphamide resin (HPR)	**0−8965**	**516**	**this work**

was proposed to explain the phenol adsorption behavior on the HPR surface. The hydrogen bonding is easy to form between the strongly electronegative oxygen atom in the P═O groups of the polymer and the strongly electropositive hydrogen atom in the hydroxyl groups (OH) of the phenol molecule.[39−41] On the other hand, the HPR is easy to swell (see Figure S2 of the Supporting Information), and the stretch of the polymer chains resulting from the HPR swelling enables more functional groups of the HPR to expose to phenol molecules and form hydrogen bonding on the its surface, which also contributes to the adsorption performance of the HPR.

If each P═O group of the HPR can interact with a phenol molecule via hydrogen bonding and the steric hindrance is not taken into account because the adjacent P═O groups can rotate to a certain extent, the phenol adsorption amount of 1 g of HPR is calculated by eq 4

$$q_{theo} = 1 \times N_{P=O} \times M_{phenol} = 1 \times 2 \times \frac{1}{M_{HPR}} \times M_{phenol} = 431 \quad (4)$$

where q_{theo} (mg g^{-1}) is the theoretical phenol adsorption amount of HPR, 1 is the number of phenol molecules combined around a P═O group, 2 is the number of P═O groups in each structure unit of HPR, $N_{P=O}$ (mol) is the mole number of P═O group in each gram of polymer, and M_{HPR} and M_{phenol} (mg mol^{-1}) are the molecular weight of structure unit of polymer and phenol, respectively.

According to the calculation above, the theoretical adsorption amount of HPR is 431 mg g^{-1}, lower than the experimental value (516 mg g^{-1}). This phenomenon is mainly attributed to the existence of N−H groups, which can also form hydrogen bonding with phenol molecules and thus adsorb phenol. However, because of the high steric hindrance in the N−H groups of the polymer matrix and the resulting difficulties for the formation of hydrogen bonding between N−H groups and phenol molecules, the amount of phenol molecules adsorbed onto N−H groups is far less than that of total N−H groups and difficult to be quantified. In addition, the increase of the surface area of the HPR caused by its swelling may also contribute to the adsorption amount. Compared to the physical adsorption model, the hydrogen binding mechanism seems to be more convincible to interpret the actual adsorption results.

4. CONCLUSIONS

A polyphosphamide resin with flexible structure for phenol adsorption was prepared. The experimental phenol-adsorption amount of this resin reached 516 mg g^{-1} in this work, within the range of those of activated carbons derived from different sources. It is worthwhile to note that the phenol-adsorption amount of HPR calculated by surface area (42.3 mg m^{-2}) is much higher than most of the activated carbon (0.102−0.827 mg m^{-2}). This excellent adsorption performance is well interpreted by the proposed chemical adsorption model and ascribed to the formation of hydrogen bonding between phenol molecules and the functional groups P═O on the HPR surface. Additionally, the flexible structure of the HPR exposes more functional groups to phenol molecules, enhancing the chemical interaction between them.

■ ASSOCIATED CONTENT

Ⓢ Supporting Information. Figure S1 shows the pH of zero point charges (pH_{PZC}) of the HPR. Figure S2 indicates the flexibility of the HPR compared to the XAD-4, a conventional adsorption resin. Figure S3 shows the XPS spectra of the HPR. Table S1 summarizes the surface area, pore volume, and size of the HPR. This material is available free of charge via the Internet at http://pubs.acs.org.

■ AUTHOR INFORMATION

Corresponding Author
*Phone/Fax: 86-551-3607482. E-mail: jhong@ustc.edu.cn.

■ ACKNOWLEDGMENT

This work was supported by the National Natural Science Foundation of China (50978242), National Water Project (2009ZX07528-006-01-02), and the Fundamental Research Funds for the Central Universities (WK2060190007).

■ REFERENCES

(1) Schwarzenbach, R.; Escher, P. B.; Fenner, I. K.; Hofstetter, T. B.; Johnson, C. A.; Gunten, U.; Wehrli, B. The challenge of micropollutants in aquatic systems. *Science* **2006**, *313*, 1072.

(2) Lian, F.; Huang, F.; Chen, W.; Xing, B.; Zhu, L. Sorption of apolar and polar organic contaminants by waste tire rubber and its chars in single- and bi-solute systems. *Environ. Pollut.* **2011**, *159*, 850.

(3) Khalid, M.; Joly, G.; Renaud, A.; Magnoux, P. Removal of phenol from water by adsorption using zeolites. *Ind. Eng. Chem. Res.* **2004**, *43*, 5275.

(4) Jiang, H.; Yu, H.-Q.; Guo, Q.-X. Extraction-oxidation-adsorption process for treatment of effluents from resin industries. *Ind. Eng. Chem. Res.* **2007**, *46*, 1667.

(5) Kubo, M.; Fukuda, H.; Chua, X.; Yonemoto, T. Kinetics of ultrasonic degradation of phenol in the presence of composite particles of titanium dioxide and activated carbon. *Ind. Eng. Chem. Res.* **2007**, *46*, 699.

(6) Bokare, A. D.; Choi, W. Zero-valent aluminum for oxidative degradation of aqueous organic pollutants. *Environ. Sci. Technol.* **2009**, *43*, 7130.

(7) Rokhina, E. V.; Makarova, K.; Golovina, E. A.; Van As, H.; Virkutyte, J. Free radical reaction pathway, thermochemistry of peracetic acid homolysis, and its application for phenol degradation: spectroscopic study and quantum chemistry calculations. *Environ. Sci. Technol.* **2010**, *44*, 6815.

(8) Nagaveni, K.; Sivalingam, G.; Hegde, M. S.; Madras, G. Photocatalytic degradation of organic compounds over combustion-synthesized nano-TiO2. *Environ. Sci. Technol.* **2004**, *38*, 1600.

(9) Ho, K. L.; Lin, B.; Chen, Y. Y.; Lee, D. J. Biodegradation of phenol using *Corynebacterium sp. DJ1* aerobic granules. *Bioresour. Technol.* **2009**, *100*, 5051.

(10) Temme, H.; Sohling, U.; Suck, K.; Ruf, F.; Niemeyer, B. Selective adsorption of aromatic ketones on kerolite clay for separation in biocatalytic applications. *Colloids Surf., A* **2011**, *377*, 290.

(11) Kim, Y.-H.; Lee, B.; Choo, K.-H.; Choi, S.-J. Selective adsorption of bisphenol A by organic-inorganic hybrid mesoporous silicas. *Microporous Mesoporous Mater.* **2011**, *138*, 184.

(12) Guo, Z.; Zheng, S.; Zheng, Z.; Jiang, F.; Hu, W.; Ni, L. Selective adsorption of p-chloronitrobenzene from aqueous mixture of p-chloronitrobenzene and o-chloronitrobenzene using HZSM-5 zeolite. *Water Res.* **2005**, *39*, 1174.

(13) Haddou, B.; Canselier, J. P.; Gourdon, C. Cloud point extraction of phenol and benzyl alcohol from aqueous stream. *Sep. Purif. Technol.* **2006**, *50*, 114.

(14) Juang, R. S.; Huang, W. C.; Hsu, Y. H. Treatment of phenol in synthetic saline wastewater by solvent extraction and two-phase membrane biodegradation. *J. Hazard. Mater.* **2009**, *164*, 46.

(15) Jiang, H.; Fang, Y.; Fu, Y.; Guo, Q. X. Studies on the extraction of phenol in wastewater. *J. Hazard. Mater.* **2003**, *101*, 179.

(16) Olejniczak, J.; Staniewski, J.; Szymanowski, J. Extraction of phenols and phenyl acetates with diethyl carbonate. *Anal. Chim. Acta* **2005**, *535*, 251.

(17) Li, P.; SenGupta, A. K. Sorption of hydrophobic ionizable organic compounds (HIOCs) onto polymeric ion exchangers. *React. Funct. Polym.* **2004**, *60*, 27.

(18) Fontanals, N.; Marce, R. M.; Borrull, F. Improved polymeric materials for more efficient extraction of polar compounds from aqueous samples. *Curr. Anal. Chem.* **2006**, *2*, 171.

(19) Zhang, W. M.; Xu, Z. W.; Pan, B. C.; Zhang, Q. J.; Du, W.; Zhang, Q. R.; Zheng, K.; Zhang, Q. X.; Chen, J. L. Adsorption enhancement of later ally interacting phenol/aniline mixtures onto nonpolar adsorbents. *Chemosphere* **2007**, *66*, 2044.

(20) Huang, J.; Huang, K.; Liu, S.; Luo, Q.; Shi, S. Synthesis, characterization, and adsorption behavior of aniline modified polystyrene resin for phenol in hexane and in aqueous solution. *J. Colloid Interface Sci.* **2008**, *317*, 434.

(21) Li, H.; Xu, M.; Shi, Z.; He, B. Isotherm analysis of phenol adsorption on polymeric adsorbents from nonaqueous solution. *J. Colloid Interface Sci.* **2004**, *271*, 47.

(22) Drechny, D.; Trochimczuk, A. W. Synthesis and some sorptive properties of highly crosslinked cyanomethyl styrene/divinylbenzene copolymers. *React. Funct. Polym.* **2006**, *66*, 323.

(23) Trochimczuk, A. W.; Streat, M.; Kolarz, B. N. Highly polar polymeric sorbents: Characterization and sorptive properties towards phenol and its derivatives. *React. Funct. Polym.* **2001**, *46*, 259.

(24) Gu, B.; Ku, Y. K.; Brown, G. M. Sorption and desorption of perchlorate and U(VI) by strong-base anion-exchange resins. *Environ. Sci. Technol.* **2004**, *39*, 901.

(25) Cichy, W.; Szymanowski, J. Recovery of phenol from aqueous streams in hollow fiber modules. *Environ. Sci. Technol.* **2002**, *36*, 2088.

(26) Zidi, C.; Tayeb, R.; Ali, M. B.; Dhahbi, M. Liquid−liquid extraction and transport across supported liquid membrane of phenol using tributylphosphate. *J. Membr. Sci.* **2006**, *360*, 334.

(27) Deng, S.; Bai, R. B. Aminated polyacrylonitrile fibers for humic acid adsorption: behaviors and mechanisms. *Environ. Sci. Technol.* **2003**, *37*, 5799.

(28) American Public Health Association, Standard Methods for the Examination of Water and Wastewater, 20th ed.; Washington DC, USA, 1999.

(29) Li, Z.; Han, J.; Jiang, Y.; Browne, P.; Knox, R. J.; Hu, L. Nitrobenzocyclophosphamides as potential prodrugs for bioreductive activation: synthesis, stability, enzymatic reduction, and antiproliferative activity in cell culture. *Bioorg. Med. Chem.* **2003**, *11*, 4171.

(30) Kannan, A. G.; Choudhury, N. R.; Dutta, N. K. Synthesis and characterization of methacrylate phospho-silicate hybrid for thin film applications. *Polymer* **2007**, *48*, 7078.

(31) Ofomaja, A. E.; Naidoo, E. B.; Modise, S. J. Kinetic and pseudo-second-order modeling of lead biosorption onto pine cone powder. *Ind. Eng. Chem. Res.* **2010**, *49*, 2562.

(32) Wu, F. C.; Tseng, R. L.; Juang, R. S. Kinetic modeling of liquid-phase adsorption of reactive dyes and metal ions on chitosan. *Water Res.* **2001**, *35*, 613.

(33) Liu, Q. S.; Zheng, T.; Wang, P.; Jiang, J. P.; Li, N. Adsorption isotherm, kinetic and mechanism studies of some substituted phenols on activated carbon fibers. *Chem. Eng. J.* **2010**, *157*, 348.

(34) Yin, J.; Chen, R.; Ji, Y.; Zhao, C.; Zhao, G.; Zhang, H. Adsorption of phenols by magnetic polysulfone microcapsules containing tributyl phosphate. *Chem. Eng. J.* **2010**, *157*, 466.

(35) Huang, J. Treatment of phenol and p-cresol in aqueous solution by adsorption using a carbonylated hyper cross linked polymeric adsorbent. *J. Hazard. Mater.* **2009**, *168*, 1028.

(36) Li, J. M.; Meng, X. G.; Hu, C. W.; Du, J. Adsorption of phenol, p-chlorophenol and p-nitrophenol onto functional chitosan. *Bioresour. Technol.* **2009**, *100*, 1168.

(37) Girods, P.; Dufour, A.; Fierro, V.; Rogaume, Y.; Rogaume, C.; Zoulalian, A.; Celzard, A. Activated carbons prepared from wood particleboard wastes: Characterisation and phenol adsorption capacities. *J. Hazard. Mater.* **2009**, *166*, 491.

(38) László, K.; Podkościelny, P.; Dabrowski, A. Heterogeneity of polymer-based active carbons in adsorption of aqueous solutions of phenol and 2,3,4-trichlorophenol. *Langmuir* **2003**, *19*, 5287.

(39) Blindheim, U.; Gramstad, T. Studies of hydrogen bonding—XV. The influence of a S---P bond in phosphoryl compounds on the P═O stretching frequency and their hydrogen bonding ability. *Spectrochim. Acta* **1965**, *21*, 1073.

(40) Kalenius, E.; Neitola, R.; Suman, M.; Dalcanale, E.; Vainiotalo, P. Hydrogen bonding in phosphonate cavitands: investigation of host-guest complexes with ammonium salts. *J. Am. Soc. Mass Spectrom.* **2010**, *21*, 440.

(41) Henn, M.; Jurkschat, K.; Mansfeld, D.; Mehring, M.; Schürmann, M. Synthesis and structure of and DFT-studies on 1,3,5-$[P(O)(i\text{-}PrO)_2]_3C_6H_3$ and its $CHCl_3$ adduct: analysis of the Cl_3C-H...OP hydrogen bond. *J. Mol. Struct.* **2004**, *697*, 213.